Bubble Capture by Large Hydrofoil Tip Vortex

R. Latorre**, J.Y Billard*, F. Moutant*, O. Roussel*
*Ecole Naval, Brest France, **Univ. of New Orleans USA

Abstract

The interaction of gas bubbles with a vortex is investigated experimentally to clarify the role of the initial bubble position on its trajectory around the tip vortex shed from a large hydrofoil. The experiments performed with 4-6mm bubbles show that the bubbles can undergo no capture, quick capture into the tip vortex or slow capture with a spiral trajectory around the vortex.

1. Introduction

Tip vortex cavitation has been the subject of a number of theoretical and experimental investigations. Arndt (1995) and Chahine(1995) One of the interesting features is the capture of nuclei into the tip vortex core Latorre (1980, 1982 Arndt and Maines 2000). A series of papers by Latorre (1980, 1982) Ligneul and Latorre (1989, 1993) present the development of their theoretical model for the behavior of spherical bubbles in the vicinity of the tip vortex. This work is the basis for the present experimental study of the bubble capture by a large hydrofoil tip vortex.

Numerical simulations of bubble growth and trajectory and subsequent theoretical analysis show the bubble capture depends on the bubble size and its distance from the vortex axis. Verification of these results in cavitation tunnel tests is complicated by high flow speeds and difficulties in resolving individual microbubble growth and trajectory paths.

To obtain experimental verification of the bubble capture by the tip vortex, experiments were performed using a large scale hydrofoil tested in the 39.3mx4.6m x 2.1m deep UNO towing tank. This paper summarizes the development of the experimental design, test procedures, and the results from the analysis of the bubble capture tests. The experiments verify bubble capture occurs and the capture is strongly dependent on the bubble position Y from the tip vortex axis.

2. Nomenclature

A	aspect ratio	-
C_D	bubble drag coefficient	
C_{max}	maximum foil chord	m
C_p	pressure coefficient	-
C_{pmin}	minimum pressure coefficient	-
$d_c(R_{b0})$	critical distance $= R/R_a$	m
Eo	bubble Eotvos number	-
g	gravitational acceleration	$m.s^{-2}$
G	Constant	
M	Bubble Morton number	-
P	local pressure	Pa
ΔP	pressure variation	-

P_G	gas pressure	Pa
P_{inf}	pressure at infinity	Pa
P_v	vapor pressure	Pa
R_1	vortex core radius	m
R_a	vortex parameter $R_a = \left[\frac{6\pi\upsilon}{\Gamma}\right]^{0.5}$	-
R	bubble radius (and derivatives)	m
R_B	bubble Reynolds number	-
Re	Reynolds number	-
Rtra, Y	bubble trajectory radius	m
S, σ	surface tension	N/m
t	time	s
V	velocity	m/s
W	fluid particle velocity vector	-
W_b	bubble velocity vector	-
X,Y,Z	vortex coordinate system	mm
α	angle of attack	-
δ	turbulent boundary layer thickness	m
η	foil span coordinate	m
μ	viscosity	Kg/m/s
ν	kinematic viscosity	m^2/s
ρ	fluid density	Kg/m^3
Δρ	density difference between gas bubble and water	Kg/m^3
Γ	vortex circulation	m^2/s
subscript o	initial condition	

3. Theoretical Model of Bubble Capture by Tip Vortex

The theoretical model of bubble capture by a tip vortex developed by Latorre (1980, 1982) is briefly reviewed. This model consists of:

1. Modeling of nuclei as spherical bubbles
2. Idealization of tip vortex as a Rankine or Oseen(Burgers) vortex
3. Analytical specification vortex circulation Γ
4. Vortex core R_1 equal to foil boundary layer thickness;
5. Model of bubble trajectory using Johnson-Hsieh formulation

The nuclei are assumed as spherical gas filled bubbles with radius R(see Section 7). The variation of the radius R with change in pressure P taken at the bubble center is given by the Rayleigh-Plesset formulation :

$$\rho(R\ddot{R}+3/2\,\dot{R}^2)=P_v-P-2S/R+G/R^3-4\mu\dot{R}/R \qquad (1)$$

The trajectory of the spherical cavitation nuclei around the tip vortex pressure field is determined by the Johnson-Hsieh formulation. This neglects the buoyancy force in the forces acting on the bubble:

$$Force = F_{Drag} + F_{\text{Pressure}} + F_{Inertial\ \ and\ \ virtual\ \ mass} \tag{2}$$

Which is written in vector form:

$$\frac{dW_b}{dt} = \frac{3}{4}\left(\overline{W} - \overline{W}_b\right)\left|\overline{W} - \overline{W}_b\right|\frac{C_D}{R} - \frac{3\nabla P}{\rho} + \frac{3}{R}\left(\overline{W} - \overline{W}_b\right)\frac{dR}{dt} \tag{3}$$

The drag coefficient C_D of the spherical nuclei is determined using Haberman's empirical equation:

$$\frac{C_D R_B}{24} = 1.0 + 0.197 R_B{}^{0.63} + 2.6x10^{-4} R_B{}^{1.38} \tag{4}$$

where:

R_B bubble Reynolds number

$$R_B = \frac{2R\left|\overline{W} - \overline{W}_b\right|}{\nu} \tag{5}$$

The model of the tip vortex flow field is a Rankine or Oseeen vortex with a characteristic circulation Γ and. core radius R_1 related to the thickness of the foil turbulent boundary layer:

$$R_1 = \delta = \frac{0.37 \cdot C_{\max}}{R_e^{0.2}}. \tag{6}$$

These equations were numerically integrated for different bubble sizes and initial position from the vortex axis. The simulations show bubble radius greater than 25 μm are captured. This capture can be characterized by the ratio of the initial bubble position Y to the vortex radius R_1 , Y/ R_1 Bubbles close to the vortex Y/ R_1 < 2 experience "quick" capture, while bubbles farther from the vortex axis experience "slow capture" characterized by a spiral around the vortex before bubble capture. This was supported by subsequent parametric analysis of these equations by Ligneul and Latorre (1989). For the case of no buoyancy force, they obtained the limiting case denoted by "critical distance".dc = R/Ra. Rtra/dc = 1 represents the limiting case between quick and slow bubble capture

3.1 Results of Bubble Capture Simulations

As part of the experimental design, a series of bubble capture simulations were performed for Foil I used in earlier cavitation tunnel tests (Latorre 1980, 1982). The parameters of Foil I are summarized in Table 1. The bubble trajectory for quick capture is shown in Fig. 1 and slow capture is shown in Fig. 2

1) Quick capture $Y/R_1 = 1.13$
Figure 1 shows the bubble position (y,z) around the vortex core and axis. This figure shows the bubble is captured with minimum rotation around the vortex This corresponds to Rtra/dc 0.67

2) Slow capture $Y/R_1 = 5.88$
Figure 2 shows the bubble position (y,z) around the vortex core and axis. This figure shows the bubble undergoes rotation around the vortex before capture. This corresponds to Rtra/dc = 3.53

4. Large Foil Experiments

The objective of the large foil experiments was to study the bubble trajectory and corresponding growth. The experimental design involved the scale-up of the test geometry of earlier 39.14-mm chord foil I tested at 12 m/s in the University of Tokyo's cavitation tunnel. (Latorre, 1980,1982). The particulars of the foil I are summarized in Table 1. This foil has a NACA 4412 foil section and an elliptic planform defined by the following equation:

$$C(\eta) = C_0 \cdot \sqrt[4]{1-\eta^2} \quad (7)$$

where $\eta = \dfrac{y}{semi-span}$

y: distance from the base.

$C_0 = C_{\max}$: chord at base.

4.1 Considerations in selecting Large foil and bubble size

Developing the large scale hydrofoil experiments involved three considerations:

1. Sizing the large hydrofoil for installation in the 5 m Jon boat test rig. This resulted in a 1.0 m base cord representinga scale ratio $\lambda = 25.54$. to Foil I.
2. Determining test speed from Reynolds scaling of Foil I test speed Vm = 12 m/s. $V = Vm/\lambda = 0.5$ m/s
3. Initial tow tank experiments showed the trajectory and growth of air bubbles with radius of 5-6 mm could be recorded by underwater video. These bubbles are relatively large corresponding to 200-300 μm microbubble radius for foil I tests.

4.2 Large Foil Design and Manufacture

The large foil was designed from a table of hydrofoil offsets used in the NC manufacture of foil I. This table of offsets consists of seven NACA 4412 sections with chord C defined by equation (7). An aluminum frame shown in Fig. 3 was designed to withstand the large foil lift and drag forces at towing speeds up to 1 m/s with the foil at an attack angle α =10 deg. The frame uses three 2.54-cm aluminum tubes with seven welded mounting plates. Seven NACA 4412 foil sections were then cut from plywood and attached to the mounting plates. The upper and lower foil surfaces were covered with 1.25-cm plywood strips screwed into the foil sections The foil's leading edge was shaped

out of foam and covered with fiber glass and epoxy resin. The foil surface was sanded and painted with waterproof marine enamel. The final check showed the large foil surface was within $\pm$ 5 mm tolerance ($\pm$0.5% of the base chord) with the foil tip being a bit flatter compared to the rounded tip of foil 1.

4.3 Large foil installation in UNO Towing tank

The large foil was mounted in a 1.25m circular base shown in Fig. 4. This foil and base assembly was then secured circular cutout in the 5 m Jon-boat bottom (Fig. 5). The circular base allowed the foil to be set at a 10 degree angle of attack within a tolerance of $\pm$0.25 degree. to restrain any side motion from the foil lift and drag forces the foil frame assembly was secured with wire to the towing carriage.

4.4 Bubble Generator and measurement field

The bubble generator system consisted of a 1.5 Hp air compressor, a two liter reservoir with 5 mm diameter plastic tubing to the bubble generator nozzles. These nozzles were fitted in a trolley moving on the tank bottom 2.1 m below the free surface. This trolley system generated large bubbles with 1.0 cm diameter. At V = 0.6 m/s, 1 cm bubbles were captured by the tip vortex when they were released at Y = 5 cm from large foil's centerline. Additional tests at different speeds showed the need to

I. Decrease the bubble radius

II. Accuraately control the bubble release location

This lead to the development of the second bubble generator replacing the trolley with a single 2.5 mm metal tube. With the tube set in the vicinity of the foil tip, (Z = 0) about 1.25 m below the free surface, the bubble size was reduced to 4-6 mm bubbles. Typically a group of 6-12 bubbles would be generated when the valve opened.

The coordinate system used to locate the bubble outlet is shown in Fig. 6. The video was focused on a dark background plate behind the large foil ($0.45<X/C<1.0$, $0.05<Y/C<0.3$). A 1 x 1 cm reference grid was attached for estimating the bubble trajectory position as well as the bubble radius.

5. Test Matrix

The large foil test matrix is summarized in Table 2. The bubble tube outlet is set following the coordinate system in Fig. 6 As Table 2 indicates, the bubble tube position was set at Y = 40, 60, and 100 mm from the foil centerline These positions correspond to $Y/R_1 < 2$, $2 < Y/R_1 < 4$ and $Y/R_1 > 4$, respectively A total of 40 tests were recorded, from which approximately 20 tests were analyzed. The most representative tests are summarized in Table 3.

6. Test Results

From the 40 tests, approximately 20 tests were analyzed. This reflects difficulties associated with bubbles moving out of the video as well as resolution at V = 1.0 m/s. The most representative tests are summarized in Table 3. This table indicates that in addition to the case of no bubble capture, the video records include both slow capture and quick capture. The distribution of bubble behavior are summarized in Fig 7 for V = 0.7 m/s and Fig. 8 for V = 0.5 m/s. The following three types of bubble behavior are shown in these figures;

1. No capture for bubble release at Y = 100 mm ($Y/R_1 = 4$ to 6)
When bubble capture does not occur, the bubble has a upward trajectory reflecting horizontal motion induced by bubble drag in the relative flow and vertical motion from the bubble buoyancy. This was predominate behavior for bubbles released at Y = 100 mm ($Y/R_1 > 4$.)

2. Quick capture for bubble release at Y = 40 mm ($Y/R_1 = 1$ to 2)
When bubble capture immediately occurs, the bubble trajectory follows a spiral with narrow loops that merges with the foil vortex core. The bubble trajectory is mainly horizontal with the vertical buoyancy motion suppressed by the capture process. This was the predominate behavior for bubbles released at Y= 40 mm ($Y/R_1 <2$)

3. Slow capture for bubble release at Y = 60 mm ($Y/R_1 = 2$ to 4)
When the bubbles are released at Y = 60 mm, ($2< Y/R_1 <4$) representing the condition between quick capture and no capture, they tend to have a large spiral trajectory before entering the vortex core. . This case is called slow capture in some cases; the bubble escapes after several loops, and follows a rising trajectory to the surface due to the buoyancy force.

7. Bubble shape
A review of bubble characteristics is given in the book of Clift et al (1978). The equilibrium spherical or elliptical bubble shape is given by Fig. 8 as a function of three parameters:

1.Bubble Reynolds Number:

$$\mathrm{Re} = \frac{2R_b V}{\nu} \qquad (7)$$

II Bubble Eotvos number:

$$Eo = \frac{g\Delta\rho(2R_b)^2}{\sigma} \qquad (8)$$

III. Bubble Morton number:

$$M = \frac{g\mu^4\Delta\rho}{\rho^2\sigma^3} \qquad (9)$$

The parameter values and corresponding bubble shape for the large foil tests are summarized in Table 4. The results indicate a spherical-elliptical bubble shape which was observed in the video records. These records showed that when the initial spherical air bubble moved in a horizontal trajectory path, it would stretch into an elliptic bubble

In contrast the analysis shows that the parameters for the microbubbles used in Foil I fall inside the spherical bubbles regime.(Table 5). This agrees with an earlier analysis done

in conjunction with the selection of the spherical bubble for the theoretical model of bubble capture (Latorre 1980, 1982).

8. Discussion and Conclusions

These large scale experiments have been useful to clarify the relationship of initial bubble location and the bubble capture by the tip vortex. The presence of bubble buoyancy and bubble rise made the determination of the non-capture and capture conditions clear. The experiment was successful in demonstrating bubble capture by the foil tip vortex.

The main conclusions from this investigation with 4- 6 mm radius bubbles are:
I. When bubbles are released at Y = 100 mm ($Y/R_1 > 4.$), their capture does not occur. The bubbles have a upward trajectory reflecting the action of bubble drag and bubble buoyancy.
2. When bubbles are released at Y= 40 mm ($Y/R_1 <2$), their capture immediately occurs, The bubble trajectory follows a spiral with narrow loops that merges with the foil vortex core. The bubble trajectory is mainly horizontal with the vertical buoyancy motion suppressed by the capture process.
3. When the bubbles are released at Y = 60 mm, ($2< Y/R_1 <4$) they tend to have a large spiral trajectory before entering the vortex core. . In small number of instances after several loops,, the bubble escapes due to the buoyancy force.
4. In these tests, the bubbles were observed as having spherical and elliptical shape. The corresponding cavitation nuclei are shown to be spherical.

The bubble growth and trajectory video records are currently being analyzed. They will be compared with the results from an expanded theoretical model which includes buoyancy to compare bubble trajectory and growth in the presence of a tip vortex. It is expected this comparison will further clarify the bubble behavior.

9. References

Ardnt R. 1995, "Vortex Cavitation," ," Green , S. Ed. FLUID VORTICES, Fluid Mechanics and Its Applications, Vol. 30, Kluwer Academic Publisher, Boston, pp. 731-782

Ardnt, R. Maines, B, 2000, "Nucleation and Bubble Dynamics in Vortical Flows", ASME Journal Fluids Engineering Vol. 122, pp 488-93

Chahine, G.L. 1995, "Bubble Interactions With Vortices," Green , S. Ed. FLUID VORTICES, Fluid Mechanics and Its Applications, Vol. 30, Kluwer Academic Publisher, Boston, pp. 783-828

Clift R., Grace J.R., Weber M.E 1978. BUBBLES, DROPS AND PARTICLES Academic Press, New York p27

Latorre, R. 1980, "Study of Tip Vortex Cavitation Noise from Foils and Propellers," International Shipbuilding Progress pp. 676-685

Latorre, R. 1982, TVC noise Envelope-An Approach to Tip Vortex Cavitation Noise Scaling," Journal of Ship Research, Vol. 26, pp 65-75

Ligneul P, Latorre, R 1989," Study on the Capture and Noise of Spherical Nuclei"

Acustica, Vol 68, pp. 1-14
Ligneul P, Latorre, R.1993, "Study of Nuclei Distribution on Capture by Tip Vortex," Journal Fluids Engineering, Vol. 117. pp. 225-232.

Parameter	Units	Large	Foil I
Scale Factor	-	25.54	1
Chord	M	1.0	0.003914
Semi-span	M	1.213	0.0050
Max thickness	M	0.106	
Foil Section		NACA 4412	NACA4412
Hydrofoil Planform	-	Elliptic	Elliptic
Aspect ratio	-	3	3
Test Speed*	m/s	0.5	12
Vortex Circulation** Γ	m^2/s	0.1011	0.1011
Vortex Core R1	Mm	27.1	1.06
Vortex parameter Ra**	-	0.0137	0.0137

Notes: * Constant Chord Reynolds Number ** Foil at 10 degrees
Table 1 Large Hydrofoil and Foil I Particulars

Test	Speed m/s	Tube Y =40	Tube Y = 60 mm	Tube Y= 100 mm
I	0.5	Yes	Yes	Yes
II	0.6	Yes	Yes	Yes
III	0.7	Yes	Yes	Yes
IV	1.0	Yes	Yes	Yes

Table 2 Large Foil Test Matrix

Test	Speed m/s	Bubble Generator	X mm	Y Mm	Z mm	Bubble motion	Observations
1	0.5	Tube	150	100	0	No capture	Trajectory of a bubble rising in a flow
2	0.5	Tube	100	60	0	Slow capture	Long spiral with large loops
3	0.5	Tube	0	40	0	Quick capture	Spiral with limited loops
4	0.6	Tube	150	100	0	No capture	Trajectory of a bubble rising in a flow
5	0.6	Tube	100	60	0	Slow capture	Long spiral with numerous loops
6	0.6	Tube	0	40	0	Quick capture	Spiral with limited loops
7	0.7	Tube	150	100	0	No capture	Trajectory of a bubble rising in a flow
8	0.7	Tube	100	60	0	Slow capture	Long spiral with numerous loops
9	0.7	Tube	0	40	0	Quick capture	Spiral with limited loops
10	1	Tube	150	100	0	No capture	Trajectory of a bubble rising in a flow
11	1	Tube	100	60	0	Slow capture	Long spiral with numerous loops
12	1	Tube	0	40	0	Quick capture	Spiral with limited loops

Table 3 Large Foil Test Results

Rb (cm)	V (m/s)	Re	Eo	log M	type of bubble	observed
0.51	0.5	4944	11.97	-10.745	ellipsoidal	spherical to ellipsoidal
0.54	0.5	5225	13.37	-10.745	ellipsoidal	spherical to ellipsoidal
0.567	0.5	5497	14.8	-10.745	ellipsoidal	spherical to ellipsoidal
0.48	0.6	5607	10.69	-10.745	ellipsoidal	spherical to ellipsoidal
0.51	0.6	5933	11.97	-10.745	ellipsoidal	spherical to ellipsoidal
0.54	0.6	6270	13.37	-10.745	ellipsoidal	spherical to ellipsoidal
0.567	0.6	3298	14.8	-10.745	ellipsoidal	spherical to ellipsoidal
0.595	0.6	6922	16.3	-10.745	ellipsoidal	spherical to ellipsoidal
0.48	0.7	6542	10.69	-10.745	ellipsoidal	spherical to ellipsoidal
0.51	0.7	6922	11.97	-10.745	ellipsoidal	spherical to ellipsoidal
0.54	0.7	7308	13.34	-10.745	ellipsoidal	spherical to ellipsoidal
0.595	0.7	8075	16.3	-10.745	ellipsoidal	spherical to ellipsoidal

Table 4. Characteristics of bubbles observed in large foil tests and predicted by Cliff et al (1978)

Rb (micron)	V (m/s)	Re	Eo	log M	type of bubble
10	10	199.3	4.60E-05	-10.79	spherical
20	6.5	259	1.84E-04	-10.79	spherical
20	8.7	346.7	1.84E-04	-10.79	spherical
20	10	398.5	1.84E-04	-10.79	spherical
25	6.5	323.8	2.88E-04	-10.79	spherical
25	8.7	433.4	2.88E-04	-10.79	spherical
25	10	498.2	2.88E-04	-10.79	spherical
30	6.5	388.6	4.14E-04	-10.79	spherical
30	8.7	520.1	4.14E-04	-10.79	spherical
30	10	597.8	4.14E-04	-10.79	spherical
50	6.5	647.6	1.15E-03	-10.79	spherical
50	8.7	866.8	1.15E-03	-10.79	spherical
50	10	996.3	1.15E-03	-10.79	spherical

Table 5. Characteristics of nuclei shape for Foil I Tests Cliff et al (1978()

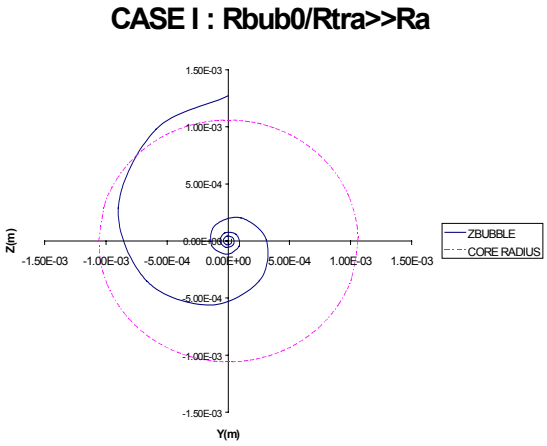

Figure 1 Numerical simulation of bubble "quick capture" by Foil I tip vortex
Rtra = 1.2 mm, Rb= 25 μm, V = 12 m/s, α=10 deg.,

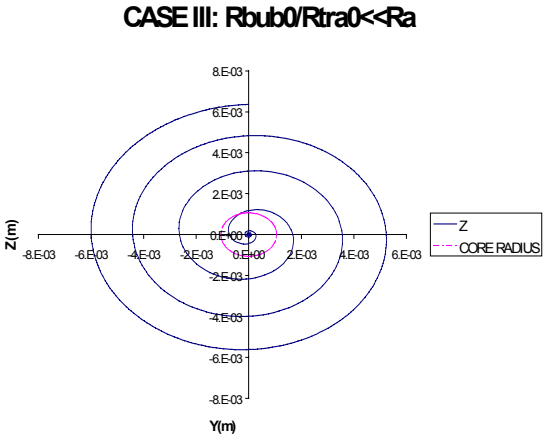

Figure 2 Numerical simulation of bubble "slow capture" by Foil I tip vortex
Rtra = 6.36 mm, Rb= 25 μm, V = 12 m/s, α=10 deg.,

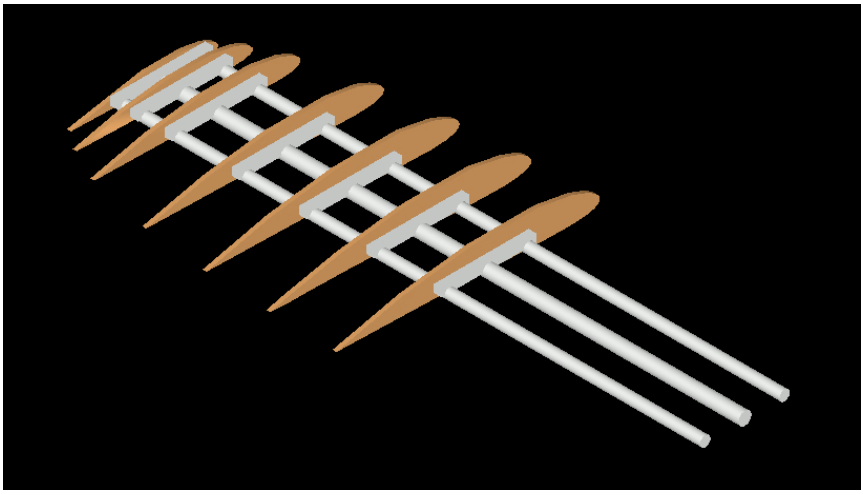

Fig.3: Schematic of the large foil frame with NACA 4412 sections.

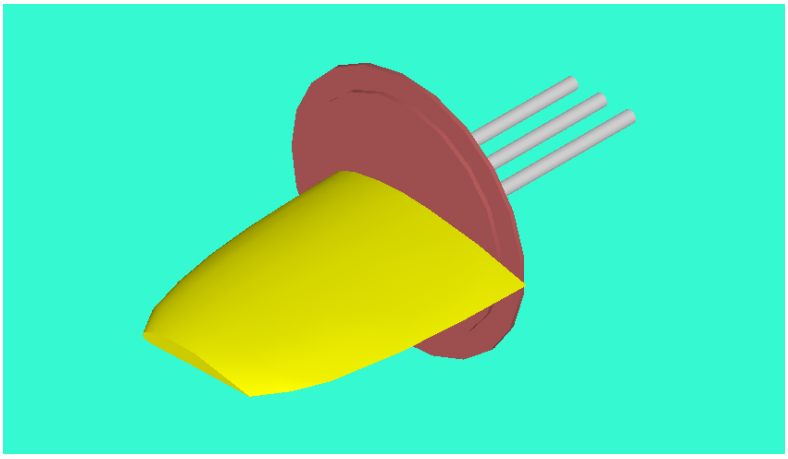

Fig. 4:Large hydrofoil on 1.25 m mounting disc

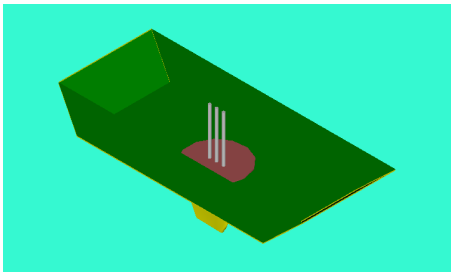

Fig. 5: Schematic of large foil installed in the 5 m Jon-Boat for the tank tests

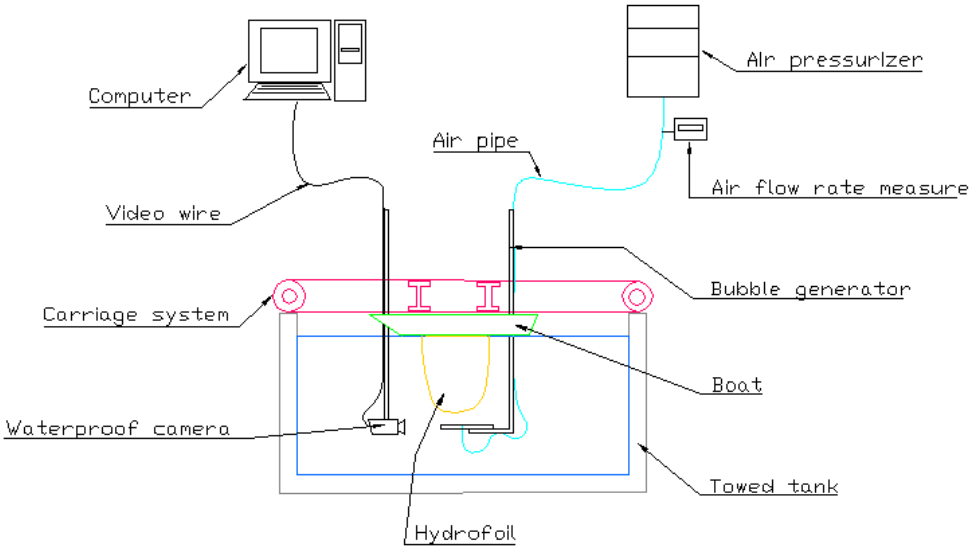

Fig. 6 Schematic showing bubble generation and bubble trajectory recording systems

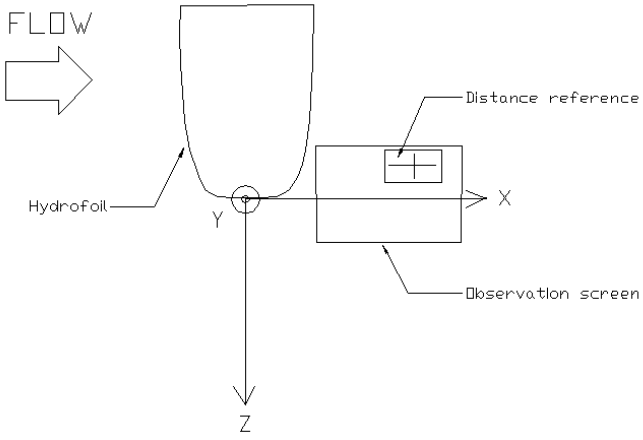

Fig. 7. Coordinate system for large foil tests

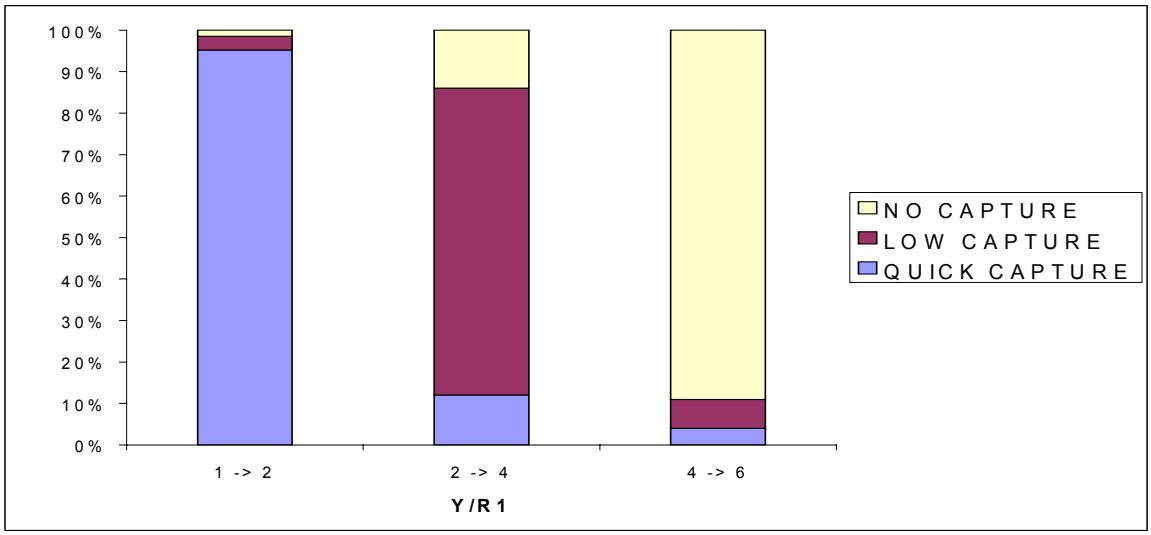

Fig. 8 Characterization of bubble behavior at V =0.5 m/s tests

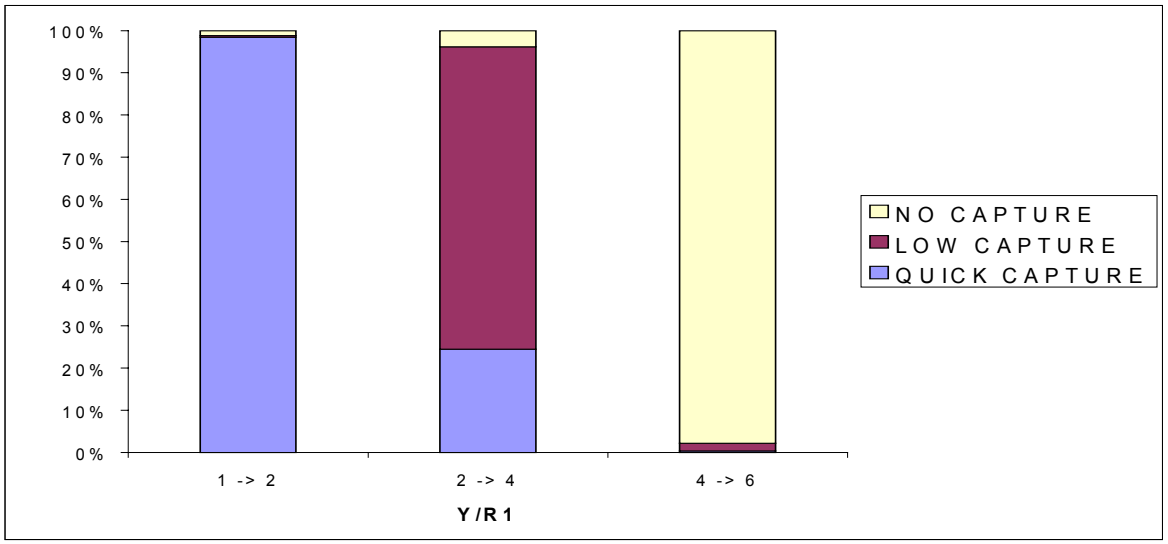

Fig. 9 Characterization of bubble behavior at V = 0.7 m/s tests

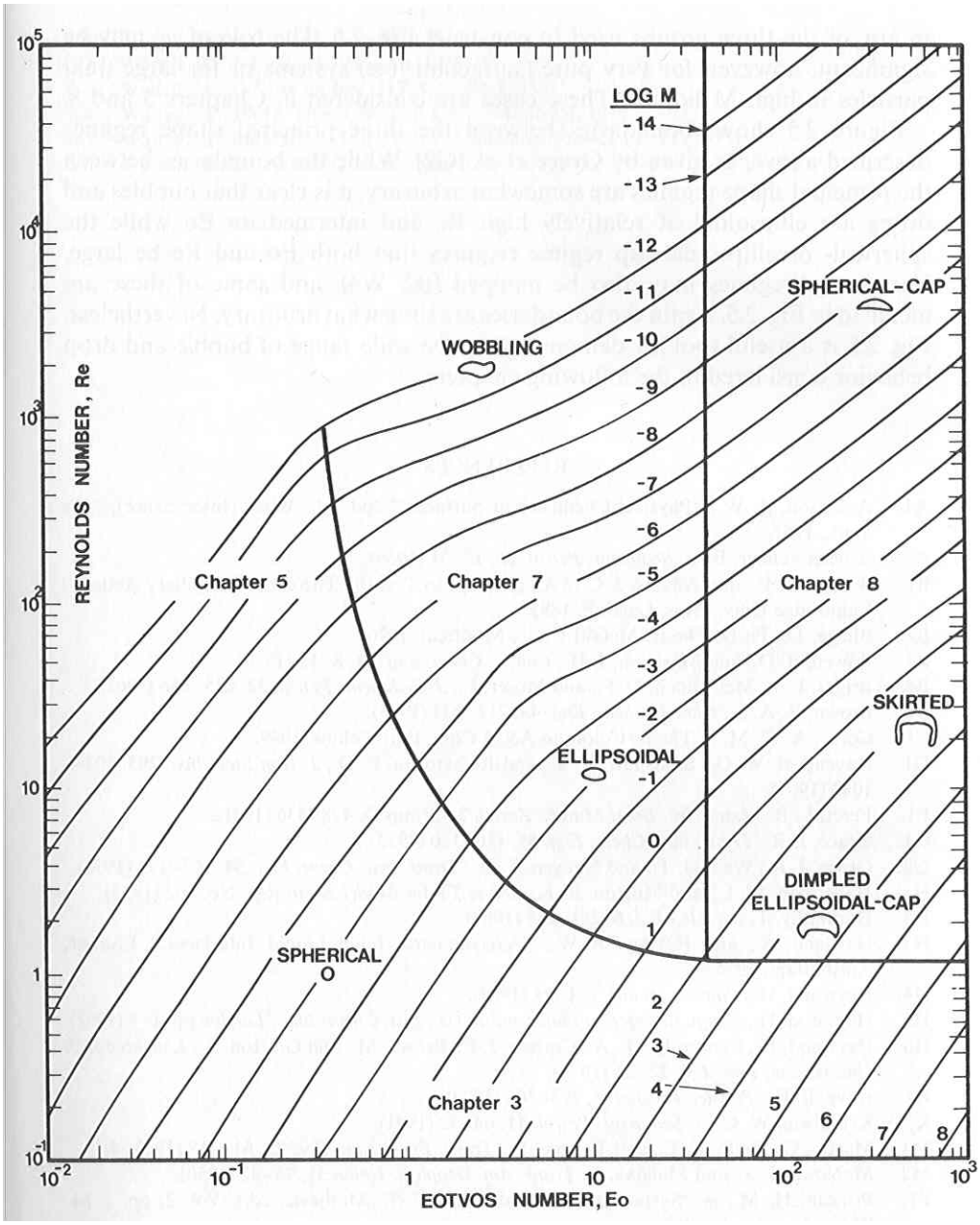

Fig. 10 Diagram of bubble shape from Clift et al. 1978